Supplemental Material for the ^{7}Be(n,p)^{7}Li paper

(available in twiki hypertexted form at the link: https://twiki.cern.ch/NTOFPublic/Be7npPaperDraft)

Adopted cross section data for R-matrix fitting

As mentioned in the paper draft, the n_TOF measurement provides cross section data for the ^{7}Be(n,p) reaction in the energy range 25 meV $\leq E_n \leq$ 325 keV. In order to perform a reliable fit of the cross section, hence to derive the corresponding reaction rate in the wide temperature range required by Big-Bang Nucleosynthesis (BBN) network calculations, we must complement the n_TOF data with data derived from the time-reversal reaction ^{7}Li(p,n)^{7}Be.

To this end, the detailed balance relation, from time-reversal invariance of strong interaction (see for example [1]),

$$\frac{\sigma_{1,2}}{\sigma_{3,4}} = \frac{k_{3,4}^2}{k_{1,2}^2}\frac{(2J_3+1)(2J_4+1)}{(2J_1+1)(2J_2+1)}\frac{(1+\delta_{1,2})}{(1+\delta_{3,4})}$$

can be used. Here, the direct and inverse reactions 1 + 2 $\leftrightarrow$ 3 + 4, are characterized by the center-of-mass momenta $k_{1,2}$ and $k_{3,4}$ and by the total angular momenta J_i of the reacting particles, while the δ's avoid double counting in the case particles 1 and 2 and/or 3 and 4 are identical. Note that this general expression simplifies to the Eq. (2) of the draft paper in the specific case of p + ^{7}Li $\rightarrow$ n + ^{7}Be(g.s.) since J_1 = J_3 = 1/2 and J_2 = J_4 = 3/2.

The data of the ^{7}Li(p,n)^{7}Be reaction from Ref. [2], transformed into ^{7}Be(n,p)^{7}Li cross section, are available here >>.

Here is a plot of the adopted data

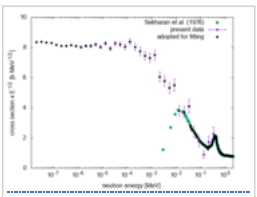

Experimental data from the ^{7}Be(n,p)^{7}Li cross section measured at n_TOF, combined with the data obtained from the time-reversal ^{7}Li(p,n)^{7}Be reaction.

A table with the numerical data, which includes the n_TOF experimental results and the data from the time-reversal reaction, is available here.

R-matrix fit of the adopted cross section

The adopted (n,p) cross section has been fitted with a single-level Breit-Wigner expression

$$\sigma_{n,p}(E_n) = \frac{\pi}{k_n^2}\sum_{r=1}^{N_r} g(J_r)\frac{\Gamma_{r,n}\Gamma_{r,p}}{(E_n-E_r)^2+\frac{1}{4}\Gamma_r^2}$$

where

$$k_n = \frac{\sqrt{2\mu c^2 E_n}}{\hbar c}, \quad g(J) = \frac{2J+1}{2(2I_t+1)}, \quad \Gamma_r = \sum_{i=n,p,\alpha}\Gamma_{r,i}.$$

μ is the reduced mass in the entrance channel and I_t the spin of the target nucleus ($I_t = 3/2$ in the present case). Both, the neutron and charged-particle widths are taken to be energy dependent in the form

$$\Gamma = 2P_l\gamma_r^2$$

where γ_r^2 is the energy-independent reduced width and can be calculated at the resonance energy, once a given width is known. The penetrability factor is given by

$$P_l(\rho) = \frac{\rho}{F_l(\rho,\eta)^2 + G_l(\rho,\eta)^2}, \quad \rho = kR, \quad \eta = \frac{Z_i Z_j e^2}{\hbar c}\sqrt{\frac{\mu_{i,j}c^2}{2E}}.$$

Here, F and G are, respectively, the regular and irregular Coulomb functions for positive energies, η the usual Sommerfeld parameter and μ the reduced mass for the entrance or exit channels, respectively in case of neutron or charged-particle widths.

A total of N_r = 9 levels (resonances) have been included in the fit of the adopted cross section data. For each resonance, the parameters available from the ENSDF library [3] have been adopted as starting values (see the table here below).

Table 1. Starting values of the resonance parameters

#	E[MeV]	Ex[MeV]	l	J	Gn[MeV]	Gp[MeV]	Ga[MeV]	Gtot[MeV]
1	0.013	18.910	0	2.0	6.100e-02	6.100e-02	0.000e+00	1.220e-01
2	0.194	19.069	1	3.0	1.000e-03	2.710e-01	0.000e+00	2.720e-01
3	0.384	19.235	1	3.0	1.140e-01	1.140e-01	0.000e+00	2.280e-01
4	0.573	19.400	0	1.0	3.200e-01	3.200e-01	0.000e+00	6.400e-01
5	1.098	19.860	3	4.0	1.000e-03	2.100e-01	4.900e-01	7.010e-01
6	1.373	20.100	1	2.0	1.000e-01	1.270e-01	5.730e-01	8.000e-01
7	1.486	20.199	1	0.0	1.500e-01	1.500e-01	3.600e-01	6.600e-01
8	2.287	20.900	2	4.0	8.000e-01	8.000e-01	0.000e+00	1.600e+00
9	3.544	22.000	0	1.0	2.000e+00	2.000e+00	0.000e+00	4.000e+00

The energies of each resonance has been kept constant while the widths have been allowed to vary. Here below is a table with the final values.

Table 2

#	E[MeV]	Ex[MeV]	l	J	Gn[MeV]	Gp[MeV]	Ga[MeV]	Gtot[MeV]
1	0.013	18.910	0	2.0	3.500e-02	1.190e-01	0.000e+00	1.540e-01
2	0.194	19.069	1	3.0	4.800e-02	4.150e-01	0.000e+00	4.630e-01
3	0.384	19.235	1	3.0	1.220e-01	7.500e-02	0.000e+00	1.970e-01
4	0.573	19.400	0	1.0	9.355e+00	3.390e-01	0.000e+00	9.694e+00
5	1.098	19.860	3	4.0	4.000e-03	4.400e-01	5.230e-01	9.670e-01
6	1.373	20.100	1	2.0	1.529e+00	1.258e+00	1.480e-01	2.935e+00
7	1.486	20.199	1	0.0	1.000e-01	1.000e-01	3.250e-01	5.250e-01
8	2.287	20.900	2	4.0	1.460e-01	1.243e+00	0.000e+00	1.389e+00
9	3.544	22.000	0	1.0	2.000e+00	2.000e+00	0.000e+00	4.000e+00

The SLBW (reduced) cross section is shown in comparison with the adopted experimental data in the figures below. Note that, most of the resonance parameters are purely fit parameters, obtained to reproduce the best representation of the adopted cross section. They are not to be considered accurate physical properties of the ^{8}Be excited states.

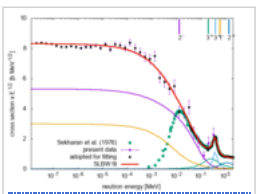

Adopted reduced (n,p) cross section shown in comparison with the SLBW fit obtained with the parameters of Table 2

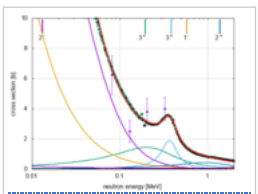

Cross section in the energy range above 10 keV

A table with the pointwise cross section calculated using the SLBW formula is provided here.

Uncertainties

Here is a table of the estimated uncertainties in the measured (n,p) cross section, all in %, with the systematics added in quadrature.

	statistical [%]	systematics [%]			
		f_C	ang. dist.	others(*)	Total
0.01 eV ≤ E ≤ 1 keV	1 - 5	8	0	5	10
1 keV ≤ E ≤ 50 keV	5 - 10	8	5 - 10	5	10 - 15
E > 50 keV		5			

(*) Including: sample mass, flux normalization and detector efficiency estimation. This component has been estimated and confirmed with the data of the measurement performed with a ^{6}Li sample (see paper text for more information).

The 5% uncertainty above E_n = 50 keV is assumed considering that the time-reversal ^{7}Li(p,n)^{7}Be cross section is know with this leve of accuracy.

New reaction rate for the ^{7}Be(n,p)^{7}Li

After a reliable fit of the (n,p) cross section σ(E) has been obtained as described in the previous section, the maxwellian averaged cross section (MACS)

$$\frac{<\sigma v>}{v_T} \equiv <\sigma> = \frac{2}{\sqrt{\pi}} \frac{1}{(kT)^2} \int_0^\infty E\sigma(E) e^{-E/kT} dE$$

can be readily calculated numerically for a full set of thermal energies *kT*. In turn, the MACS can be promptly converted into a reaction rate

$$N_A <\sigma v> = 10^{-24} <\sigma> 6.022 \times 10^{23} \times 3 \times 10^{10} \sqrt{\frac{2kT}{\mu c^2}} =$$

$$= 2.457 \times 10^8 \sqrt{\frac{A_1 + A_2}{A_1 A_2}} <\sigma> \sqrt{T_9}$$

in units of cm^3/s/mole when <σ> is in barn and the temperature T_9 in 10^9 degrees. The numerical results can be accurately described by the following analytical expression [4], which includes a power expansion in T_9 (coefficients a_0 to a_5) plus an exponential term (a_6), as well as a resonance term (a_7)

$$N_A <\sigma v> = a_0(1 + a_1 T_9^{1/2} + a_2 T_9 + a_3 T_9^{3/2} + a_4 T_9^2 + a_5 T_9^{5/2}) +$$

$$+ a_6 \left(\frac{1}{1 + 13.076 T_9}\right)^{3/2} + a_7 T_9^{-3/2} e^{-b_0/T_9}$$

in units of cm^3/s/mole when a_0= 6.805e+09, a_1= -1.971e+00, a_2= 2.042e+00, a_3= -1.069e+00, a_4= 2.717e-01, a_5= -2.670e-02, a_6= 1.963e+08, a_7= 2.889e+07, and b_0= 2.811e-01.

A code segment (in c) with the expression above is given here

```
/* Be7 + n -> p + Li7 */
/* rate from n_TOF  - central value */
        a0=   6.8048e+09; a1= -1.9706e+00; a2=  2.0419e+00; a3= -1.0687e+00; a4=  2.7172e-01; a5= -2.6699e-02; a6=  1.9610e+08; a7=  2.8899e+07; b0=  2
        rrate = a0*(1. + a1*pow(T9,1./2.) + a2*T9 + a3*pow(T9,3./2.) + a4*T9*T9 + a5*pow(T9,5./2.)) + a6*pow(T9/(1.+13.076*T9),3./2.)/pow(T9,3./2.) + a
```

Considering now that the reaction rate is linear with the maxwellian averaged cross section, the reaction rate with its uncertainty can be estimated. The result is shown in the figure below, where a comparison of the reaction rates for the ^{7}Be(n,p)^{7}Li reaction of the present work with some of the commonly adopted rates ([4], [5], [6]) with respect to the rate of Cyburt (2004) [7]. The uncertainty associated with the presently determined rate is shown by the corresponding grey band. The temperature range of interest for BBN is indicated by the vertical band.

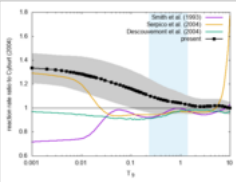

This figure is equivalent to Figure 3 of the draft paper, with the addition of the error bars in the present data, estimated as described in the text.

The reaction rate in tabular form can be found here.

Implications on the BBN

The calculations of the BBN yields have been performed using an updated version of the AlterBBN code of Alexander Arbey *et al.* [8] where the 12 most important rates have been updated.

Details of the reaction rates used are given here >>.

As mentioned in the paper draft, the BBN calculations have been performed adopting a neutron average life-time of $\tau_n = 880.2$ s and $N_\nu = 3$ neutrino species. The baryon-to-photon number density ratio η_{10} (in units of 10^{-10}) has been allowed to vary within the uncertainty quoted in the CMB analysis and in the wider range established by the concordance of observation of primordial ^{4}He and deuterium as evaluated in the review of the most recent Particle Data Group publication [9]. The results of the BBN calculation for the main observables are shown in the following table.

	Y_p	D/H [10^{-5}]	^{3}He/H [10^{-5}]	^{7}Li/H [10^{-10}]
present with standard rates	0.246	2.43	1.08	5.46
present with new rate (η_{10} = 6.09)	0.246	2.43	1.08	5.26 ± 0.40
present with new rate (5.8 ≤ η_{10} ≤ 6.6)	0.246	2.43	1.08	4.73 - 6.23
observations	0.245 ± 0.003	2.569 ± 0.027	-	1.6 ± 0.3

The uncertainty or range of variation of the Lithium production is associated *only* to the corresponding variation of the ^{7}Be(n,p)^{7}Li reaction rate uncertainty.

A typical plot of the ^{7}Li and ^{7}Be yields, plotted vs η are shown here. Similar plots for Y_p, D and ^{3}He are here.

Calculations performed with an updated version of L Kawano's code *NUC123* [10] produced results of all the yields practically identical to those obtained with the AlterBBN code, once the reaction rates (and the Cosmology parameters) have been set the same.

(n,p) and (p,n)

Time-reversal invariance, mentioned above, can be invoked to derive the ^{7}Li(p,n)^{7}Be cross section from the present ^{7}Be(n,p)^{7}Li measured cross section data. Here below is a plot of the derived (p,n) cross section.

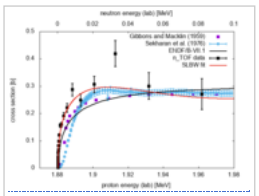

^{7}Li(p,n)^{7}Be near threshold

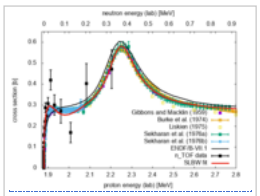

^{7}Li(p,n)^{7}Be in the full energy range up to E_p = 2 MeV

A comparison is shown here with the data of Gibbons and Macklin [11] and Sekharan *et al.* [2], in the left panel, while a more complete set, available from the EXFOR database are shown on the right panel. The ENDF/B-VII.1 [12] data are plotted as well. The SLBW cross section, calculated with the resonance parameters of Table 2 above, is plotted as well.

Both, direct and time-reversal data, are provided here >> in tabular form.

Q&A

Q: The ^{7}Be(n,p)^{7}Li is actually *producing* ^{7}Li. How come that a higher rate for this reaction results in a lower ^{7}Li yield?

A: The ^{7}Be(n,p)^{7}Li reaction is producing ^{7}Li, while destroying ^{7}Be. However, during BBN, the ^{7}Li is readily consumed by the ^{7}Li(p,α) reaction. Therefore, the net result of the ^{7}Be(n,p)^{7}Li process is a reduction of the ^{7}Be yield. In the end, the ^{7}Be that survives BBN, will undergo electron-capture decay

$$^{7}\mathrm{Be} + e^{-} \rightarrow ^{7}\mathrm{Li} + \nu_e.$$

More than 95% of final cosmic ^{7}Li abundance is, in fact, due to the survival of ^{7}Be during BBN. Therefore, an increase in the rate for the ^{7}Be(n,p)^{7}Li reaction results in a reduction of the ^{7}Li abundance.

See also the Q&A below.

Q: Could you provide a time/temperature evolution plot of the BBN yields obtained with the adopted parameters and reaction rates?

A: Certainly. Here it is (**click on the image** or **reload the page** to see the time evolution):

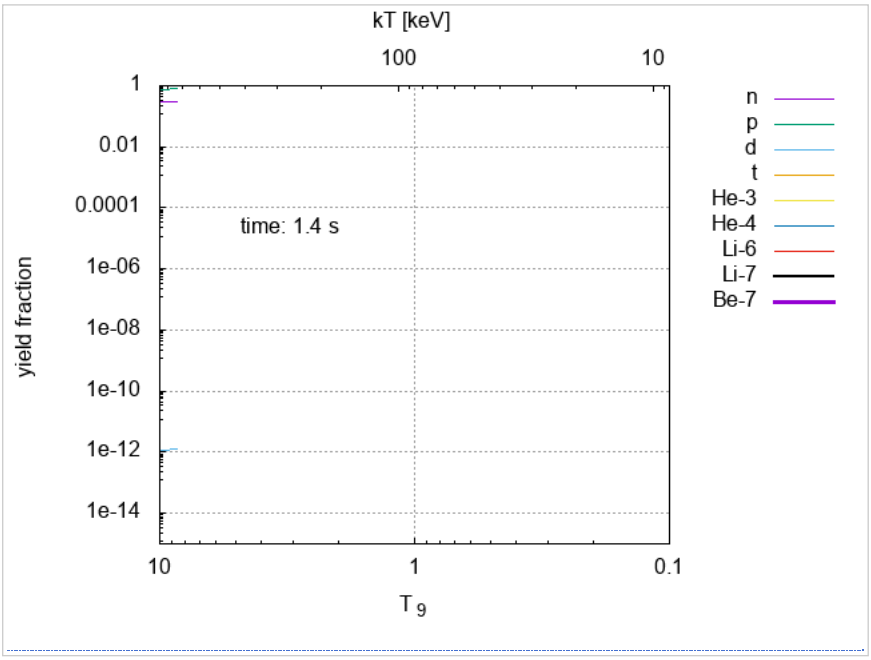

Q: Have you considered the contribution of the (n,p_1) component to the ^{7}Be(n,p)^{7}Li cross section?

A: Yes. The first exited state in ^{7}Li at 478 keV has a spin and parity $J^\pi = 1/2^-$ (see figure below).

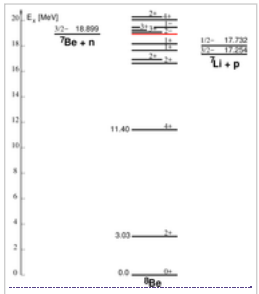

Energy levels for ^{7}Be, ^{8}Be, and ^{7}Li relevant for the (n,p) and (p,n) reactions.

Therefore, if a $J^\pi = 2^-$ is formed by s-wave neutron on ^{7}Be, the state cannot decay into ^{7}Li(1st) by emitting *l=0* (no sufficient angular momentum), nor *l=1* (no parity conservation) protons. Because the 2^- state just above threshold in ^{8}Be dominates the reaction mechanisms in a wide energy range, it is possible to estimate the (n,p_1) contribution to the ^{7}Be(n,p)^{7}Li cross section by calculating the ration of penetrabilities of *l=2* to *l=0* protons in the p + ^{7}Li(1s) exit channel. The result of this estimate is shown in the figure below.

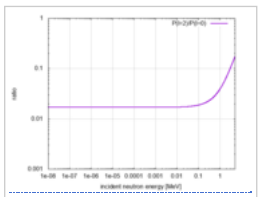

Estimate of the (n,p_1) contribution to the ^{7}Be(n,p)^{7}Li cross section.

Considering the simplicity of the assumption, this estimate is compatible with the experimental value quoted by Koehler *et al.* [13] of (1.2 ± 0.5)%.

Q: Why the (n,p) reaction taking place in the ^{14}N contained in the backing is not producing background at low neutron energies?

A: In order to identify the protons in the ΔE-E telescope, the protons must have an energy > 1.2 MeV. In the case of the ^{14}N(n,p) reaction, at least E_n > 500 keV must be added to the the Q-value of 625 keV to generate protons with enough kinetic energy to go through the ΔE detector.

Q: You did not cite our paper on a CLiP solution or attempted solution. Why?

A: A Scholarly Article google search for the *Cosmological Lithium Problem* (CLiP) produced 9,920 items, as of today (13 March 2018). Here is a table with a very few (arbitrarily) selected examples.

Category	Description	CLiP solved	Reference
nuclear/non-standard physics	non-maxwellian velocity distribution during BBN	yes	S. Q. Hou *et al.*, ApJ 834 (2017) 165. pap
nuclear physics	^{7}Be beta-decay rate in hot plasma	no	S. Simonucci *et al.*, ApJ 764 (2013) 118. doi
non-standard physics	massive gravitino particle decay	maybe	R. H. Cyburt *et al.*, JCAP 10 (2010) 32. pdf
non-standard physics	sterile neutrino, decaying after BBN	yes	L. Salvati *et al.*, JCAP (2016) 2. pdf
astronomy	interstellar lithium observations	no	J. C. Howk *et al.*, Nature 489 (2012) 121. doi
nuclear physics	trojan horse method for reaction rate determination	no	R. G. Pizzone *et al.*, ApJ 786 (2014) 112. pap
non-standard physics	exotic late-decaying particles with lifetimes exceeding ~1 sec	yes	D. Cumberbatch *et al.* Phys. Rev. D **76** (2007) 123005. pap
...			

If you send in a reference, we can add it to this table.

References

1. Claus E. Rolfs, William S. Rodney, *Couldrons in the Cosmos*, University of Chicago Press, 1988
2. K.K.Sekharan, H.Laumer, B.D.Kern, F.Gabbard, *A neutron detector for measurement of total neutron production cross sections*, Nuclear Instruments and Methods in Physics Res. **133** (1976) 253. doi.
3. D.R. Tilley and J.H. Kelley and J.L. Godwin and D.J. Millener and J.E. Purcell and C.G. Sheu and H.R. Weller, *Energy levels of light nuclei A=8,9,10*, Nuclear Physics **A745** (2004) 155. doi, url.

4. M.S. Smith, L. Kawano, and L.H. Malaney, *Experimental, computational, and observational analysis of primordial nucleosynthesis*, The Astrophysical Journal **85** (1993) 219. url.
5. P. Descouvemont, A. Adahchour, C. Angulo, A. Coc, and E. Vangioni-Flam, *Compilation and R-matrix analysis of Big Bang nuclear reaction rates*, Atomic Data and Nuclear Data Tables **88** (2004) 203. doi
6. P.D. Serpico, S. Esposito, F. Iocco, G. Mangano, G. Miele, and O. Pisanti, *Nuclear reaction network for primordial nucleosynthesis: a detailed analysis of rates, uncertainties and light nuclei yields*, Journal of Cosmology and Astroparticle Physics **12** (2004) 10. doi
7. Cyburt, Richard H, *Primordial nucleosynthesis for the new cosmology: Determining uncertainties and examining concordance*, Phys. Rev. D **70** (2004) 023505. doi
8. A. Arbey, *AlterBBN: A program for calculating the BBN abundances of the elements in alternative cosmologies*, Computer Physics Communications **183** (2012) 1822. url, doi.
9. C. Patrignani *et al.* (Particle Data Group), *Big-Bang Nucleosynthesis* (review), Chin. Phys. C **40** (2016) 100001. url pdf
10. L. Kawano, *Primordial Nucleosynthesis - The Computer Way*, FERMILAB-Pub-92/04-A (1992). pdf.
11. J.H. Gibbons, and R.L. Macklin, *Total Neutron Yields from Light Elements under Proton and Alpha Bombardment*, Phys. Rev. **114** (1959) 571. doi, url
12. M. Chadwick *et al.*, *ENDF/B-VII.1 Nuclear Data for Science and Technology: Cross Sections, Covariances, Fission Product Yields and Decay Data*, Nuclear Data Sheets **112** (2011) 2887. doi, url.
13. P.E. Koehler, C.D. Bowman, F.J. Steinkruger, D.C. Moody, G.M. Hale, J.W. Starner, S.A. Wender, R.C. Haight, P.W. Lisowski, and W.L. Talbert, Phys. Rev. C **37** (1988) 917. url.

-- AlbertoMengoni for the n_TOF Collaboration - 2018-02-13

List of the 12th most important reactions in the BBN network

	code index	reaction	adopted	options
1	12	$^1H(n,\gamma)D$	ando	ando skm
2	16	$^3He(n,p)T$	stlb	stlb de04 skm
3	17	$^7Be(n,p)^7Li$	ntof	ntof cy04 skm
4	19	$^7Be(n,\alpha)^4He$	ntof	wag ntof
5	20	$D(p,\gamma)^3He$	il16	il16 skm
6	24	$^7Li(p,\alpha)^4He$	stlb	stlb cf88 de04 skm
7	26	$T(\alpha,\gamma)^7Li$	stlb	stlb skm
8	27	$^3He(\alpha,\gamma)^7Be$	il16	il16 ncr2 skm cd08
9	28	$D(d,n)^3He$	stlb	stlb skm
10	29	$D(d,p)T$	stlb	stlb skm
11	30	$T(d,n)^4He$	stlb	stlb de04 cf88 skm
12	31	$^3He(d,p)^4He$	stlb	stlb de04 skm

```
#wag  : Wagoner, R.V., ApJS, 18, 247 (1969)
#cf88 : Caughlan and Fowler, ADNDT 40, 283 (1988)
#skm  : Smith, Kawano and Malaney, ApjS 85, 2019 (1993)
#de04 : Descouvemont et al. ADNDT 88, 203 (2004)
#cy04 : Cyburt, PRD 70, 023505 (2004)
#ando : Ando et al. Phys. Rev. C 74, 025809 (2006)
#il16 : Iliadis et al., ApJ 831, 107 (2016)
#ncr2 : fit to ncare2 library
#stlb : fit to starlib table
#ntof : rate from n_TOF experiments
```

Code segments of the individual reaction rates adopted in the present BBN calculations

Reaction 12 $^1H(n,\gamma)D$ plot table

```
/* H + n -> g + H2 */
/* rate from Ando et al. Phys. Rev. C 74, 025809 (2006) */
/* p + n -> d + g */
        a0 = 44216.0; a1 = 3.75191; a2 = 1.92934; a3 = 0.746503; a4 = 0.0197023; a5 = 3.00491e-6;
        b1 = 5.4678; b2 = 5.62395; b3 = 0.489312; b4 = 0.00747806;
        f[12]=a0*(1. + a1*T9 + a2*pow(T9,2.) + a3*pow(T9,3.) + a4*pow(T9,4.) + a5*pow(T9,5.))/(1. + b1*T9 + b2*pow(T9,2.) + b3*pow(T9,3.) + b4*pow(T9,4
```

Reaction 16 $^3He(n,p)T$ plot table

```
* He3 + n -> p + H3 */
/* starlib rate parameters -  de04 data */
        a0 = 6.89423e+08;   a1 = -0.4347;      a2 = -0.199323;    a3 = 0.590373;     a4 = -0.322449;    a5 = 0.0742735;    a6 = -0.00648816;
        f[16] = a0*(1. + a1*pow(T9,1./2.) + a2*T9 + a3*pow(T9,3./2.) + a4*pow(T9,2.) + a5*pow(T9,5./2.) + a6*pow(T9,3.));
```

Reaction 17 $^7Be(n,p)^7Li$ table

```
* Be7 + n -> p + Li7 */
/* rate from n_TOF  - central value */
        a0=   6.8048e+09; a1= -1.9706e+00; a2=  2.0419e+00; a3= -1.0687e+00; a4=  2.7172e-01; a5= -2.6699e-02; a6=  1.9610e+08; a7=  2.8899e+07; b0=  2
        f[17] = a0*(1. + a1*pow(T9,1./2.) + a2*T9 + a3*pow(T9,3./2.) + a4*T9*T9 + a5*pow(T9,5./2.)) + a6*pow(T9/(1.+13.076*T9),3./2.)/pow(T9,3./2.) + a

/* rate from n_TOF  - upper */
        a0=   6.8181e+09; a1= -1.6226e+00; a2=  1.4457e+00; a3= -6.7629e-01; a4=  1.5737e-01; a5= -1.4373e-02; a6=  7.3135e+08; a7= -2.8413e+08; b0=  8
        f[17] = a0*(1. + a1*pow(T9,1./2.) + a2*T9 + a3*pow(T9,3./2.) + a4*T9*T9 + a5*pow(T9,5./2.)) + a6*pow(T9/(1.+13.076*T9),3./2.)/pow(T9,3./2.) + a

/* rate from n_TOF  - lower */
        a0=   7.5185e+09; a1= -2.4307e+00; a2=  2.9935e+00; a3= -1.7338e+00; a4=  4.6746e-01; a5= -4.7572e-02; a6= -9.7708e+08; a7= -7.0378e+09; b0=  3
        f[17] = a0*(1. + a1*pow(T9,1./2.) + a2*T9 + a3*pow(T9,3./2.) + a4*T9*T9 + a5*pow(T9,5./2.)) + a6*pow(T9/(1.+13.076*T9),3./2.)/pow(T9,3./2.) + a
```

Reaction 19 $^7Be(n,\alpha)^4He$ table

```
/* Be7 + n -> a + He4 */
/* n_TOF rate as in Barbagallo et al. PRL 117 (2016) 152701 */
        f[19]=4.81e+5 + 1.84e+6*T9 + 3.03e+6*pow(T9,1.5);
```

Reaction 20 $D(p,\gamma)^3He$ plot table

```
/* H2 + p -> g + He3 */
/* rate from Iliadis et al. (2016) fit */
        a0=    2.452e+03; b0=    3.732e+00; a1=  -1.632e+00; a2=   7.609e+00; a3=  -6.133e+00; a4=   6.557e+00; a5=  -1.042e+00;
        f[20]=a0*pow(T9,-2./3.)*exp(-b0*pow(T9,-1./3.))*(1. + a1*pow(T9,1./3.) + a2*pow(T9,2./3.) + a3*T9 + a4*pow(T9,4./3.) + a5*pow(T9,5./3.));
```

Reaction 24 $^7Li(p,\alpha)^4He$ plot table

```
/* Li7 + p -> a + He4 */
/* starlib rate parameters -  de04 data */
        a0 = 1.45251e+09;    b0 = 8.44454;       a1 = -6.76368e+08;  b1 = 8.41908;       a2 = 4.0217e+09;    b2 = 25.3862;       b3 = 0.16592;
        f[24] = a0/pow(T9,2./3.)*exp(-b0/pow(T9,1./3.)) + a1*pow(T9/(1.0+b3*T9),5./6.)/pow(T9,3./2.)*exp(-b1/pow(T9/(1.0+b3*T9),1./3.))+a2/pow(T9,3./2.
```

Reaction 26 $T(\alpha,\gamma)^7Li$ plot table

```
/* H3 + a -> g + Li7  original */
/* starlib rate parameters -  in17 data */
        a0=   1.3350e+05; b0=  8.0768e+00; a1=  5.9164e+00; a2= -1.3045e+01; a3=  1.3315e+01; a4= -6.4673e+00; a5=  1.3420e+00; a6=  5.1090e+05; b1=  8
        f[26]=a0/pow(T9,2./3.)*exp(-b0/pow(T9,1./3.))*(1.+a1*pow(T9,1./3.)+a2*pow(T9,2./3.) + a3*T9 + a4*pow(T9,4./3.) + a5*pow(T9,5./3.)) + a6*pow(T9/
```

Reaction 27 $^3He(\alpha,\gamma)^7Be$ plot table

```
/* He3 + a -> g + Be7 */
/* rate from Iliadis et al. (2016) fit */
        a0=   9.8079e+06; b0=   1.4192e+01; a1= -1.3272e+00; a2=  1.9911e-01; a3=  1.0387e+00; a4= -6.7320e-01; a5=  1.2511e-01; a6=  6.1164e+06; b1=
        T9F=T9/(1.+0.1071*T9);
        f[27]= a0*pow(T9,-2./3.)*exp(-b0/pow(T9,1./3.))*(1.+a1*pow(T9,1./3.) + a2*pow(T9,2./3.) + a3*T9 + a4*pow(T9,4./3.) + a5*pow(T9,5./3.)) + a6*pow
```

Reaction 28 $D(d,n)^3He$ plot table

```
/* H2 + H2 -> n + He3 */
/* starlib rate parameters -  in17 data */
        a0 = 3.95e+8; b0 = 4.259; a1 = 0.098; a2 = 1.00239; a3 = 1.08419; a4 =-0.743092; a5 = 0.139404;
        f[28]=a0*pow(T9,-2./3.)*exp(-b0/pow(T9,1./3.))*(1.+a1*pow(T9,1./3.)+a2*pow(T9,2./3.)+a3*T9+a4*pow(T9,4./3.)+a5*pow(T9,5./3.));
```

Reaction 29 $D(d,p)T$ plot table

```
/* H2 + H2 -> p + H3 */
/* starlib rate parameters -  in17 data */
        a0 = 4.12649e+08; b0 = 4.258; a1 = 0.304711; a2 = -0.446767; a3 = 2.23021; a4 = -1.19482; a5 = 0.210592;
        f[29]= a0*pow(T9,-2./3.)*exp(-b0/pow(T9,1./3.))*(1.+a1*pow(T9,1./3.)+a2*pow(T9,2./3.)+a3*T9+a4*pow(T9,4./3.)+a5*pow(T9,5./3.));
```

Reaction 30 $T(d,n)^4He$ plot table

```
/* H3 + H2 -> n + He4 */
/* starlib rate parameters -  de04 data */
        a0 = 6.32853e+10; b0 = 4.52388; b1 = 0.072028;      a1 = 6.47865;       a2 = -29.3575;      a3 = 4.35456;       a4 = 280.001;       a5 = -253.094;
        f[30]=a0*pow(T9,-2./3.)*exp(-b0/pow(T9,1./3.)-pow(T9/b1,2.))*(1. + a1*pow(T9,1./3.) + a2*pow(T9,2./3.) + a3*T9 + a4*pow(T9,4./3.) + a5*pow(T9,5
```

Reaction 31 $^3He(d,p)^4He$ plot table

```
/* He3 + H2 -> p + He4 */
/* starlib rate parameters -  de04 data */
        a0 = 2.46165e+10; b0 = 7.15127; b1 = 0.241809; a1 = 8.69492; a2 = -22.7967; a3 = 21.7527; a4 = 6.97; a5 = 34.9149; a6 = 4.82217e+08; b2 = 1.713
        f[31]=a0*pow(T9,-2./3.)*exp(-b0/pow(T9,1./3.)-pow(T9/b1,2.))*(1.+ a1*pow(T9,1./3.)+ a2*pow(T9,2./3.) + a3*T9 + a4*pow(T9,4./3.) + a5*pow(T9,5./
```

-- AlbertoMengoni - 2018-02-20

This topic: NTOFPublic > WebPreferences > Be7npPaperDraft > Be7npPaperDraftRates
Topic revision: r10 - 2018-05-14 - AlbertoMengoni